

■ ORIGINAL PAPER ■

Temperature Distribution Measurement during Low Temperature Reaction in Auto-ignition Process

KAMARRUDIN, Nur Saifullah^{1,3*}, TAKAHASHI, Shuhei¹, and IHARA, Tadayoshi²¹ Graduate School of Engineering, Gifu University, 1-1 Yanagido, Gifu, 501-1193, Japan² Gifu University, 1-1 Yanagido, Gifu, 501-1193, Japan³ Universiti Malaysia Perlis, Pauh Putra Main Campus, Arau, Perlis, 02600, Malaysia

Received 8 July, 2014; Accepted 15 November, 2014

Abstract : An experimental study was performed to evaluate measurement of temperature development behavior for auto-ignition process in Rapid Compression Machine simulating a HCCI engine. In the experiments, n-heptane was used as the fuel and the charge mixture was compressed in homogeneous manner with varying compression ratio. Infrared emission method was used to capture the temperature distribution and CO₂ gas was used as the emission medium, as CO₂ has strong emission band near 4.3-4.5 μ m. The emitted radiation was recorded by a high speed infrared camera. The relationship between the emitted energy and the medium temperature was calculated with RADCAL code, and the database for different pressures and temperatures within relevant ranges to engine combustion was prepared in advance. The obtained results show that the temperatures in the cylinder were not uniform due to a roll-up vortex right after the compression. The difference in the temperature distribution behavior at different equivalence ratio during the ignition delay was successfully captured. The developed technique could be applied for detecting the slight temperature change due the low temperature reaction and the motion of the charge.

Key Words : Temperature distribution, Emission, Carbon dioxide, HCCI, Rapid compression machine

1. Introduction

A homogeneous charge compression ignition (HCCI) engine is proposed to be a new developing engine due to its diesel-like process producing high thermal efficiency while offering lower NO_x [1]. HCCI strongly relies on auto-ignition mechanism which is caused by chemical kinetics of the charge inside being compressed adiabatically. However, major problem of HCCI is that rapid pressure rise causes knock especially in high load conditions, which limit the operation range of the engine. The knock is strongly affected by the slight temperature change in the charge, and it is important to measure and control the temperature profile in the cylinder.

In the previous study [2, 3] using n-heptane as the fuel in rapid compression machine (RCM) to demonstrate knock phenomenon in an engine showed that the conditions in which knock occurred were determined as a function of compression ratio and the temperature reached after the compression. However, knock phenomenon was not guaranteed to be occurred even with the same compression ratio and equivalence ratio; thus

its reproducibility relied on the slight change in the initial condition. Here the temperature in the cylinder was assumed to be uniform within a short compression period. However, our previous experimental study with a high speed camera [4-6] reported that there was a motion of the gas that seemed to have different temperature than the surroundings even in the simple geometry of RCM. The movement of a piston along the cylinder wall peels off the cold gas in the boundary layer on the cylinder wall and mixes it with the hot gas in core region; this phenomenon is known as a roll up vortex. The roll up vortex was observed as a ring shape shadow during the combustion process. Most of the cases, it was expected that this roll up vortex was approximately 20K-40K lower than the temperature of the surrounding mixture with the compression ratio of 8.7 [5]. If the temperature difference due to the roll-up vortex becomes significant, it would affect the knock phenomenon considerably because the typical temperature range in HCCI engine conditions is near the so-called negative temperature coefficient (NTC) region. Thus the temperature profile inside the RCM may be one of the reasons why knock reproducibility were sensitive. However, such sensitivity is characteristic feature of the HCCI, and it is important issue to detect the slight change in temperature

* Corresponding author. E-mail: saifullah@unimap.edu.my

profile in the cylinder. Therefore, measurement of temperature profile will be focused in this paper and nonintrusive method is preferable.

Recently, optical diagnostics has been main interest such as measurement of flow field, soot particles and gas temperature in an engine cylinder. For measuring gas temperature, there are numbers of popular method such as laser induced fluorescence (LIF) [7], Rayleigh scattering method [8], and diode laser absorption method [9]. However, these methods required at least two optical windows at different location for allowing laser beam pass through to detector, which caused system setup complicated as well as expensive laser system. Moreover, they are still difficult to be applied to high pressure environment like a combustion chamber of RCM due to the nature of their relatively weak signal. Other measurement methods are infrared method using absorption/radiation medium such as H₂O or CO₂, which is suitable for engine combustion [10]. As for infrared emission method, only one window is necessary, which is suitable for engine combustion. The disadvantages of the infrared emission method however are as follows; 1) the emission intensity from the gas could be insufficient if the temperature is near TDC condition, 2) the profile of the emitted intensity from high temperature medium gas still has uncertainty, and 3) the high speed infrared camera was not available in past.

In our previous study, we developed two-band infrared emission method for stable combustion field and succeeded in obtaining temperature distribution [11]. In the present study, we measured the temperature distribution in the RCM from the time at the top dead center (TDC) position till the time where rapid pressure rise due to the thermal flame was observed; the period of ignition delay. The fuel was n-heptane, and the duration of the target process was approximately within 10 msec. In order to obtain the history of temperature profile, we doped small amount of CO₂ in the charge and measured the emission energy from CO₂ by a high speed infrared (HSIR) camera. Recent development in optical measurement apparatus enables us to monitor the high-speed change within infrared wave length range. We first verified the accuracy of the technique developed, and then applied it for measuring the temperature profile during the ignition delay.

2. Experiment Setup

2.1. Rapid Compression Machine (RCM)

In the experiments, RCM was used to measure temperature distribution in the cylinder after TDC. Although the behavior of the gas motion and the composition of the charge in RCM are different from those in the practical reciprocating engine, RCM can simulate a single compression process and maintain constant volume after compression; therefore it allows easy measurements

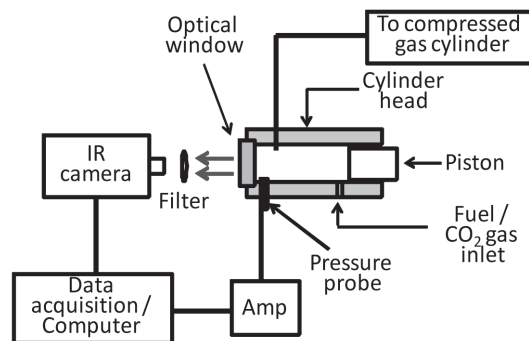


Fig.1 Schematic of experimental apparatus.

of ignition delay and emission intensity through the window. Additional advantage is that absence of intake and exhaust valves avoid the complicated gas motions such as swirl or tumble that exist in a practical engine.

The RCM used here has 65mm bore and 142mm stroke. The compression ratio (CR) was changeable, mainly set to be 10.0 – 12.0. The charge was supplied through the inlet port. First the cylinder was evacuated by the pump, and the fuel, n-heptane, was injected into the cylinder by micro-syringe, and then the air was introduced. The initial pressure was 0.101MPa. The charge was then compressed with an aluminum piston driven by high pressure air. The compression time was approximately 30ms, which correspond to the rotation speed of 1000rpm. A pressure transducer (KISTLER 6052C) was used to monitor the pressure history in the cylinder from the beginning of compression until 30ms after TDC. A high speed infrared camera (FLIR SC7000) was used to capture the IR emission from CO₂ inside combustion chamber, which was finally converted to the temperature. The frame rate of the HSIR camera was 3598 fps. The cell size of the detector was 30 μ m. The size of measurement area was 85mm x 68mm, which corresponded to 80 x 64 pixels in this article. Therefore, the corresponding area for a cell was about 1.1mm square.

The radiation from CO₂ was filtered by a narrow band pass filter (center wavelength 4428nm, width \pm 57nm) located in front of the HSIR. An optical trigger which detects the motion of the piston was used to synchronize the zero-time for both the pressure transducer and the HSIR. Since this experiment involves IR optical measurement, a sapphire glass was used as an optical window placed on the top of the cylinder head. The arrangement of experiment apparatus is illustrated in Fig. 1. For temperature measurement, small amount of CO₂ (4.0 vol%) as the IR emitter medium gas was doped in the cylinder from the inlet port by a micro-syringe.

2.2. Infrared Emission Method

Carbon dioxide has strong emission band around 4.3 μ m and

its spectrum profile changes depending on the number density and the temperature. In the emission method, we detect the emitted energy through a narrow band pass filter. Additionally, our target, which is compressed mixture undergoing low temperature reaction, does not produce CO_2 in the low temperature reaction before the thermal flame appears. Therefore, CO_2 is a good medium for the measurement. In order to calculate temperature with the emission method, the database of emitted energy from CO_2 in the relevant ranges of pressure and temperature should be prepared. The radiation spectrum from CO_2 around $4.3\mu\text{m}$ is due to asymmetric stretching mode of C-O bond. There have been developed several radiation calculation codes, for example, HITRAN, HITEMP, which are based on line-by-line calculations. The alternative approach is the statistical one, for example, RADCAL [12], which uses the narrow band model based on the theory proposed by Malkmus [13]. Although line-by-line approach has high resolution, the accuracy at higher temperature ($>1000\text{K}$) is not so good due to the lack of experimental data [14]. On the other hand, RADCAL is based on the result of combustion experiments and, therefore, its spectrum profile has moderate accuracy even at high temperature [15]. The present emission method depends especially on the shape of the spectrum within the width of the filter but not on the integrated intensity, as mentioned later. Hence, RADCAL code is preferable for the present method. Therefore, the database used to reconstruct the gas temperature was built by RADCAL, in which the self-absorption by the layers which were located between the detector and the gas under consideration, namely, the effect of the optical thickness was considered properly. For experiment with $\text{CR}=11$, the physical thickness was set to be 14.5mm , and the optical thickness was calculated by the thickness, pressure and CO_2 concentration. Of course, the HSIR camera would detect the integral of the intensity along the optical path. Therefore, if the complex distribution exists along the path, it causes reasonable error. In the present article, we assumed that the profile along the path was simple top hat distribution due to the simple geometry of the cylinder.

In order to convert the signal from the IR camera to the gas temperature, we calibrated the relation between the emission energy and the reported temperature of the HSIR camera used. Following steps were done to measure HSIR emission and is illustrated in Fig. 2. First we measure direct radiation from simulated black body i.e. a ceramic heater with non-reflective black paint coating. A thermocouple was placed behind ceramic heater and connected to the temperature controller in order to keep the heater's temperature steady. The temperatures of the ceramic heater were set to be from $600\text{K} - 900\text{K}$ with increasing every 10K . These temperatures labeled as T_{ref} . HSIR then were set to capture the corresponding temperature of the heater, which are labeled as T_{bb} . Emission energy from black body (ceramic

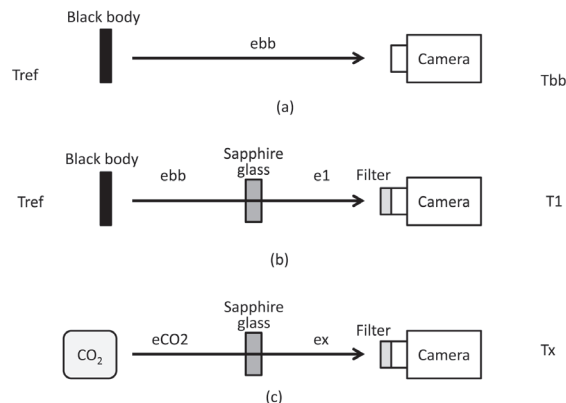


Fig.2 Calibration method for measuring emission intensity from CO_2 .

heater) at specific temperature can be calculated based on Planck theory, e_{bb} . Since some portion of the emission was absorbed by atmosphere, the reported temperature T_{bb} would result in lower value than T_{ref} . Hence, the relation between actually emitted energy, e_{bb} and the temperature of the heater, T_{ref} will be established first. This step is illustrated in Fig. 2(a).

Next, the same process as mentioned above was repeated, but at this time the sapphire glass and the narrow band pass filter were installed between the light source and HSIR camera as shown in Fig. 2(b). As expected, recorded temperature in thermal camera is getting much lower as emitted radiation from blackbody was limited by the sapphire glass and the narrow band pass filter. The recorded temperature at HSIR camera is designated as T_1 . The transmittance of the sapphire glass and the narrow band-pass filter were investigated by Fourier transform infrared (FTIR) spectroscopy in advance, therefore the emission energy that reaches the HSIR camera, e_1 , could be calculated from e_{bb} . Therefore, new relation between e_1 and T_1 was then obtained, which was used to estimate the gas temperature.

The process in Fig. 2(c), shows how we estimate the emission energy released from CO_2 gas, e_{CO_2} . Recorded temperature at HSIR camera was named as T_x and the emission captured was noted as e_x . With the relation between e_1 and T_1 , we can calculate e_x from T_x . When e_x is known, then e_{CO_2} also can be calculated from the transmittances of the glass and the filter. Finally radiation emission of e_{CO_2} can be extract from T_x . Once e_{CO_2} is known, corresponding temperature of CO_2 can be calculated based on database created from RADCAL code. Therefore, the accuracy of the developed method mainly depended on the model that RADCAL code used, but its validity has confirmed by Modest et al. [15].

The typical spectrum profile of radiation from CO_2 at several given temperatures, and the transmittance of the band-pass filter used in the experiments are shown in Fig. 3. The selected band (center wavelength 4428nm , width $\pm 57\text{nm}$) is located on the slope where the emission intensity begins to fall off. In our

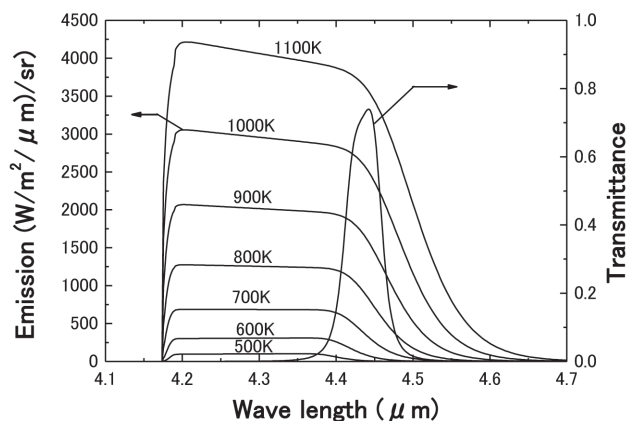


Fig. 3 Predicted emission intensity profile from compressed CO₂ at different temperature. Pi = 0.101 MPa and the CR = 11.0.

previous research [16], it was found that if the band is located at shorter wave length near 4.2-4.3 μm, the absorption in the cold boundary layer on the glass became large, which caused considerable error. On the other hand, if the band was set at further wave length, the intensity at low temperature was so small that we could not measure the profile at low temperature condition. Therefore, the band for the measurement should be selected properly according to the temperature and pressure ranges relevant to the measured object.

Integrating the specific spectrum profile at a given temperature with the transmittances of the glass and the band pass filter, we obtain the amount of emission captured by IR camera, e_x ; the HSIR camera captures the emission from the CO₂ through the band-pass filter and the sapphire glass. Fig. 4 shows an example of the predicted relation between the temperature of CO₂ and the detected infrared intensity for the condition where the initial pressure is 0.101 MPa and the CR = 11.0. We calculate such curves from the database with varying the total pressure, CO₂ concentration and the thickness of the clearance volume, which are changed according to the compression ratio and the initial pressure. Based on this information, we are able to calculate specific temporal temperature of CO₂ from T_x reported by HSIR camera.

3. Experimental Results and Discussion

3.1. Temperature Measurement at TDC Condition without Combustion

The accuracy of the calculated temperature at TDC were checked by experiments with RCM of two different conditions i.e. 1) air and CO₂ gas (4.0 vol%); 2) nitrogen gas, CO₂ gas (4 vol%) and n-heptane (corresponding $\phi = 0.4$, if the air was used) as fuel. The other experimental parameters were the compression ratio (CR) to be 10.0, 11.0 and 12.0, the initial pressure (Pi) set to be at 0.101 MPa, and the initial temperature (Ti) to be 298K. The

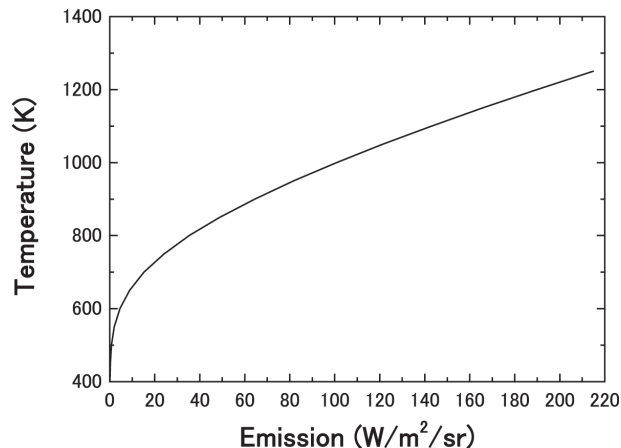


Fig. 4 Relation between the temperature of CO₂ and the detected infrared intensity through band-pass filter and sapphire window. Pi = 0.101 MPa and the CR = 11.0.

amount of CO₂ gas was determined so that sufficient emission intensity could be captured by HSIR camera at TDC condition [17].

Fig. 5(a) shows the temperature distributions at TDC for CR of 11.0. The contour lines were drawn by interpolation with the surrounding measurement points. The charge is air including 4 vol% CO₂. The temperature data are converted from the emission of the medium gas captured by HSIR camera. It can be seen that there is a lower temperature ring-shape region between the center and the cylinder wall. This region is difficult to be recognized at TDC condition, however when the temperature increases due to the low temperature reaction, the region will appear clearly as ring shape pattern as shown later. This shape is known as roll-up vortex. Depending on the experiment parameters, the temperature inside roll-up vortex usually recoded to be up to 30K lower compared with the surroundings. When the initial temperature, T_i , was 298K, the calculated polytropic and adiabatic temperature in the cylinder was 732K and 755K respectively. The polytropic index was calculated from pressure history and the compression ratio. The measured temperature was distributed from 724.7K to 741.7K, and the core temperature, which is 736K, is between the adiabatic and polytropic temperatures.

The TDC temperature for nitrogen and n-heptane mixture ($\phi = 0.4$) including 4 vol% CO₂ are shown in Fig. 5(b). The CR is 11.0. The calculated polytropic and adiabatic temperatures were 699K and 730K respectively. The measured temperature inside the cylinder shows the temperature distribution in the range from 697.9K to 711.0K. Based on the above mentioned data, it is found that these experimental values agreed well with the estimated temperature from the pressure data.

The obtained T_{TDC} were plotted in Fig. 6(a) and (b). The maximum and minimum temperatures in the measured area are plotted for comparison with the adiabatic temperature and the

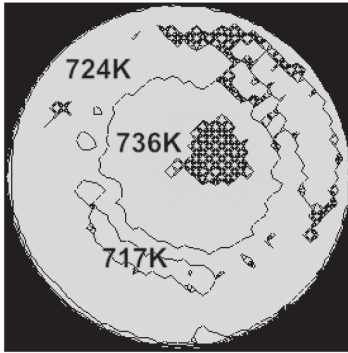


Fig. 5(a) Temperature distribution inside combustion cylinder with contours every 10 K. Compression mixture: air and CO₂ (4.0 vol%). $P_i = 0.101\text{MPa}$, $T_i = 298\text{K}$ and $CR = 11.0$.

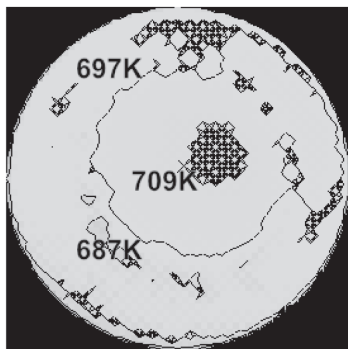


Fig. 5(b) Temperature distribution inside combustion cylinder with contours every 10 K. Compression mixture: nitrogen, CO₂ (4.0 vol%) and n-heptane ($\phi = 0.4$). $P_i = 0.101\text{MPa}$, $T_i = 298\text{K}$ and $CR = 11.0$.

polytropic temperature calculated from the pressure history. The adiabatic process takes account of the temperature dependence on the ratio of specific heats. In Fig. 6(a), T_{TDC} increases with CR monotonically. The maximum T_{TDC} for CR=10.0 are slightly over than adiabatic process, whereas the maximum T_{TDC} for CR=12.0 recorded lower value than the polytropic temperature. Although the results contain such errors, the obtained temperature was reasonable because the maximum temperature was between the adiabatic temperature and the polytropic temperature. For fuel including mixture, nitrogen gas which have similar specific heat ratio with air was used as the inert gas instead of air, to avoid auto-ignition reaction during the compression. In Fig. 6(b), the effect of low specific heat ratio of n-heptane are obvious; the temperature is significantly lower about 30K-40K. For fuel-N₂ mixture, the accuracy of the obtained temperature is also reasonable.

3.2. Temperature Measurement during Ignition Delay

In the present study, CO₂ gas is essential as the medium gas to measure the temperature, and we doped a small amount of CO₂ in the cylinder. Although CO₂ is one of the major species in the

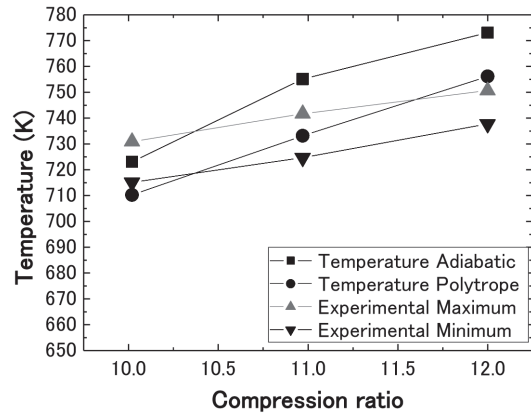


Fig. 6(a) Comparison between experimental data and calculated temperature at TDC for adiabatic and polytropic processes with three different CRs. The charge was Air-CO₂ (4 vol%).

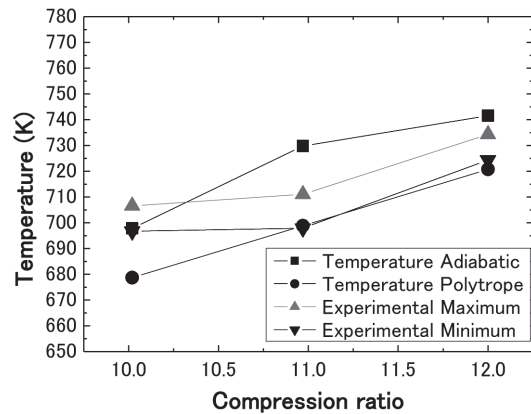


Fig. 6(b) Comparison between experimental data and calculated temperature at TDC for adiabatic and polytropic processes with three different CRs. The charge was N₂-CO₂ (4 vol%)-n-heptane ($\phi = 0.4$).

residual gas in engines, it is important to investigate the effect of the doping CO₂ on the ignition delay. Fig. 7 shows pressure histories after the TDC for compression gas charge with and without CO₂. The lower curve is the pressure through the low-pass filter and the upper graph is the pressure through high-pass filter. The equivalence ratio is 0.7 and the amount of the CO₂ is 4 vol%. The compression ratio is 10.0. The effects of doping CO₂ into the charge are as follows; 1) the maximum pressure increase from 7.94 MPa (without CO₂) to 8.59 MPa, i.e. about 8.2%, and 2) the ignition takes place about 0.6 ms later with CO₂. It is thought that these differences result from the effect of CO₂ that suppresses the low temperature kinetics like EGR process [18]. We measure the Knock Intensity (KI) from the high frequency signal by the manner proposed by Konig et al.[19], which is define as

$$KI = \frac{1}{N} \sum_{i=1}^N (p'_i - p'_{mean}) \quad (1)$$

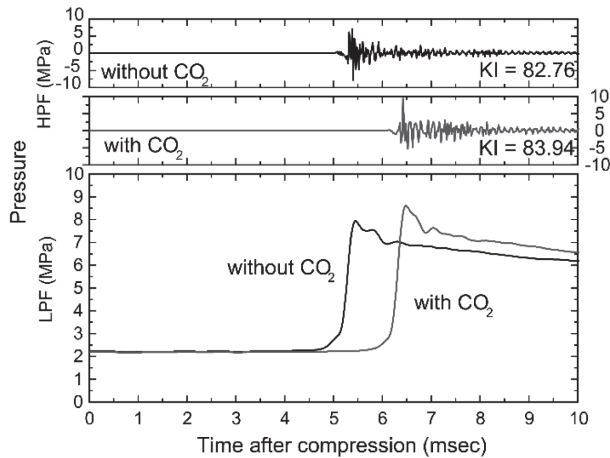


Fig. 7 Effect of doping CO₂ in-cylinder on homogeneous combustion process using n-heptane as a fuel. Experiment condition for with CO₂: P_i = 0.101MPa, T_i = 299K, ϕ = 0.7. Without CO₂: P_i = 0.101MPa, T_i = 299, ϕ = 0.7.

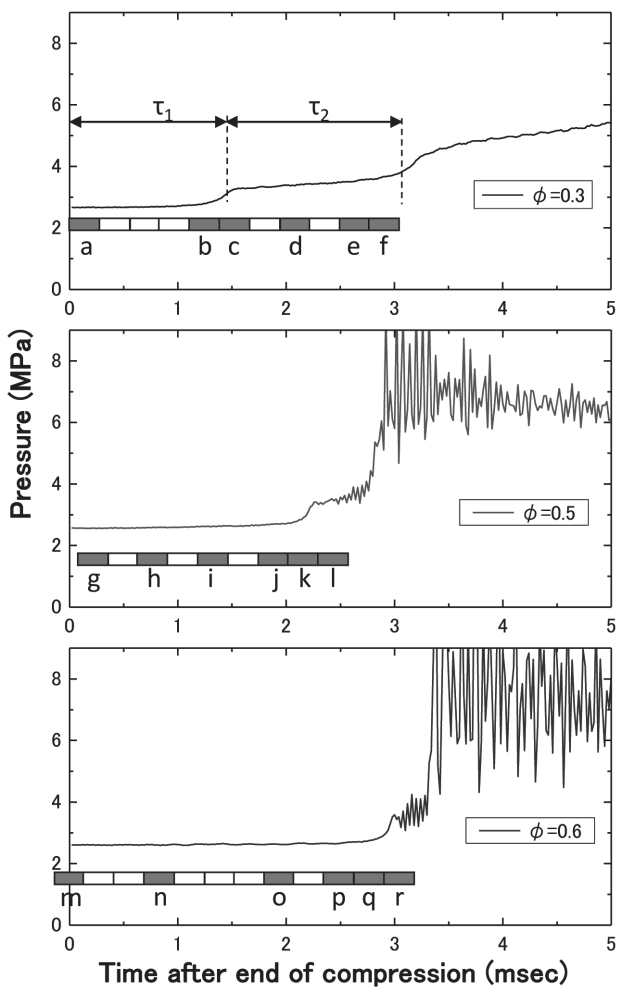


Fig. 8 Pressure histories at ϕ = 0.3, 0.5 and 0.6 of n-heptane-air-CO₂ mixture in RCM. P_i = 0.101MPa, T_i was set approximately 298K. The compression ratio was 11.0.

The KI for the mixture without CO₂ is 82.76 while that with CO₂ is 83.94. Overall, the effect of the CO₂ is small and does not totally change the auto-ignition phenomenon.

Next, we carried out the experiments with three different equivalence ratio (ϕ), i.e. 0.3, 0.5 and 0.6. The initial pressure is 0.101MPa, and the CR is 11.0, with the initial temperature is 298K. The pressure profiles for these experiments were shown in Fig. 8. For a leaner ϕ of 0.3, so-called two stage ignitions occurred and it could be seen from two times increment of pressure trace. Almost no pressure oscillation was observed, and therefore knocking does not occurred in this condition. For the richer condition, (ϕ = 0.6), it is observed that combustion process complete in almost single ignition (accompanied with very short second ignition delay), with heavy knock intensity comparing with other experiments. Here we adopted the well-used definition that the ignition delay till the cool flame appears as τ_1 , and the delay after τ_1 till the thermal flame appears as τ_2 as seen in Fig. 8. The τ_1 was shortest for ϕ = 0.3, and was longest for ϕ = 0.6. On the other hand, the τ_2 has opposed trend to τ_1 . This is a well-known trend in the NTC region [20], and it is thought that the observed result comes from the difference in the equivalence ratio and the temperature at TDC due to the difference in the specific heat ratio.

Fig. 9 shows the temperature distribution inside the cylinder after TDC, which corresponded to the experiments shown in Fig. 8. The indexes (a)-(r) in Fig. 9 were correspond to the frame bar labeled in Fig. 8. The results shown here agreed with our previous study [4-6] that the temperature distribution right after TDC does exist, which is caused by the movement of the piston during the compression process. Furthermore, a ring-shape pattern known as a roll up vortex becomes clear as the temperature increase.

For lower ϕ , the T_{TDC} of the mixture should have higher value because it has higher specific heat ratio. Fig. 9 shows the consistent results; T_{TDC} = 726K for ϕ = 0.3 (Fig. 9a), T_{TDC} = 714K for ϕ = 0.5 (Fig 9g), and T_{TDC} = 704K for ϕ = 0.6 (Fig 9m), respectively. The results are consistent with the theoretical anticipation.

As shown in Fig. 8, there occurred two stage ignition for ϕ = 0.3 and 0.5. Then we verified the temperature during low temperature reaction in these cases. The pressure in the cylinder for ϕ = 0.3 increased from 2.67Mpa to 2.80MPa at t = 1.35ms, increased to 3.39MPa at 2.19ms and then gradually increased to 3.52MPa till 2.74ms as shown in Fig. 8. Assuming the constant volume process, the calculated temperatures at 1.35ms, 2.19ms and 2.74ms are 761K, 922K and 958K, respectively, if the initial core temperature was assumed as 726K as shown in Fig. 9(a). The corresponding measured temperature within τ_1 period increased from 726K to 767K at t = 1.35ms, and increased to 915K at 2.19ms, and finally reached 944K at 2.74ms. The estimated core temperature (T_{core}) at each frame is shown in Fig. 9. T_{core}

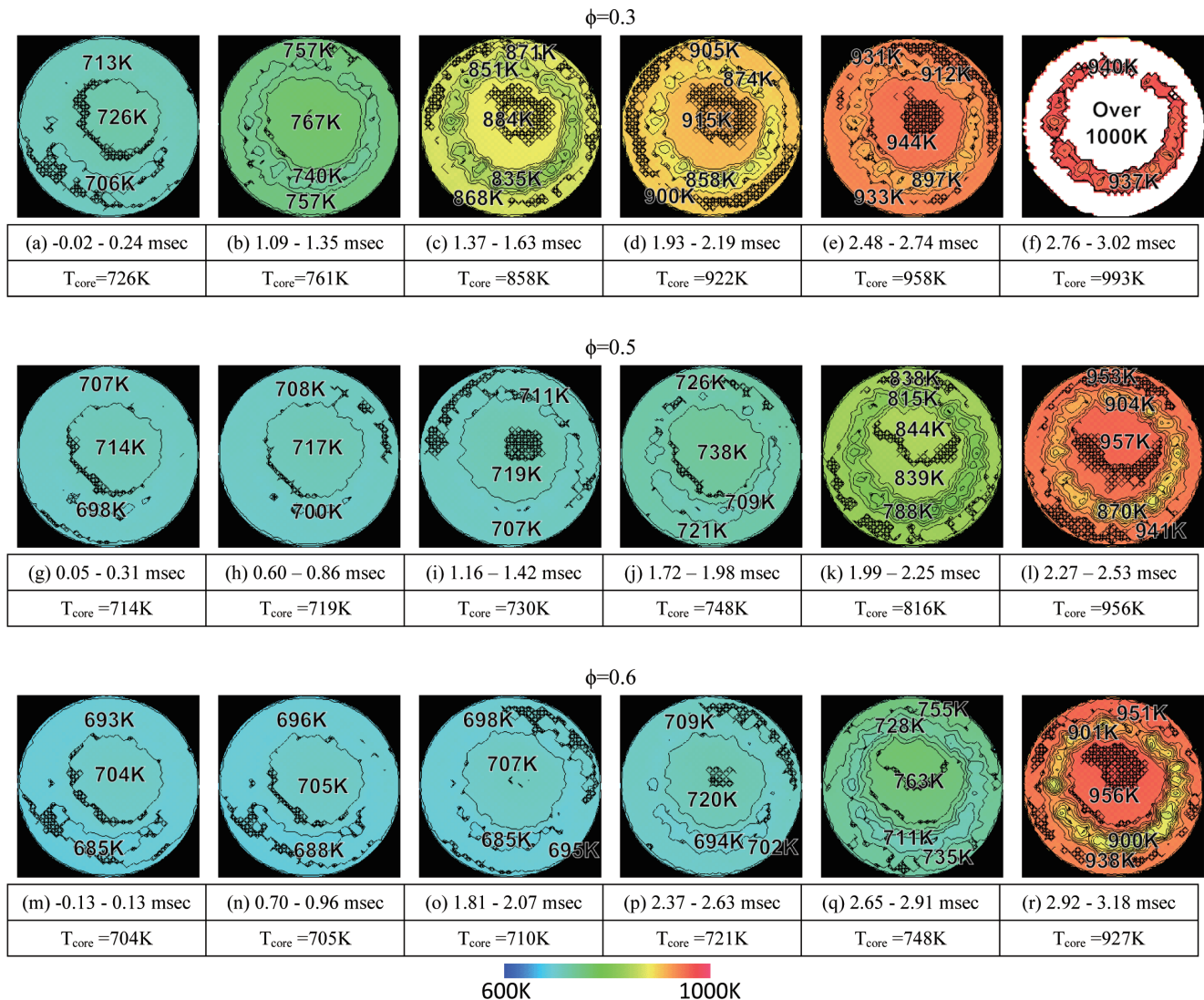


Fig. 9 Temperature distribution obtained with infrared emission method with contours every 10 K. $\phi = 0.3, 0.5$ and 0.6 . $P_i = 0.101\text{MPa}$, and T_i was set approximately 298K . The predicted temperatures from the pressure histories in Fig. 8 are also shown.

was defined as temperature located near the center of the cylinder so that effect of roll up vortex and the heat loss to the side wall were assumed to be negligible. In this experiment, T_{core} was defined to be within 20mm in diameter size from center of cylinder. The T_{core} at TDC (refer Fig. 9(a), (g) and (m)), were the temperature which was obtained by the emission method developed. Therefore the absolute value may contain some error. The rest core temperatures after TDC in Fig. 9 were calculated by pressure history with the assumption that the volume kept constant. Thus, the obtained core temperatures agreed with the estimation quantitatively, and also the results give information of temperature distributions.

As shown in Fig. 9(f), it is found that there is white region inside of cylinder which indicates over 1000K . According to the pressure history in Fig. 8, the thermal flame begins to appear at the moment. Therefore, in Fig. 9(f), huge radiation is released,

and additionally the amount of CO_2 increases as combustion products. As the amount of CO_2 increased to some unknown value than the initial concentration, the temperature after this time is out of the target of this study

For $\phi = 0.5$, after the relatively long τ_1 period, the pressure increased from 2.56MPa to 3.44MPa , and after a short time the rapid pressure rise due to the thermal flame appeared. The estimated temperature during τ_2 is 956K , and the temperature in Fig. 9(l) is 957K , which agrees with the estimation.

For $\phi = 0.6$, longer τ_1 period is observed due to low T_{TDC} . The temperature during τ_1 period is almost the same till $t = 2.63\text{ms}$. After that the temperature slightly increased due to the beginning of low temperature reaction (Fig. 9(q)), then the thermal flame follows after very short τ_2 .

In all conditions, the obtained temperature and the calculated core temperature were consistent, and the infrared emission

method could distinguish the temperature difference about 10K in the cylinder. However, when the pressure change was rapid or pressure oscillation occurred during the exposure time, such as Fig. 9(c), (k) and (r), the difference between the core temperature and the obtained temperature became large. The rapid change of temperature during the camera exposure time could cause reasonable error in the calculated temperature.

4. Conclusions

An experimental study was conducted to measure the temporal temperature distribution in RCM by applying the infrared emission method with 4.3 μ m band of carbon dioxide. As the results, the followings are concluded.

1. The temperature of the no-reacting charge with varying the compression ratio and that adding the fuel agreed with the theoretical estimation. The developed temperature measurement technique could distinguish the temperature difference about 10K. Additionally the characteristics temperature distribution due to the movement of the piston called a roll up vortex was successfully captured. The results showed that temperature at roll up vortex region was 10-30K lower than the core temperature.
2. The temporal behavior of the temperature profile of the reacting charge in the cylinder during the ignition delay was successfully captured. Not only the temperature change due to the appearance of cool flame but also the gradual temperature increasing during the low temperature reaction were captured quantitatively as two-dimensional information. Such information is useful for interpret the auto-ignition phenomena of the compressed charge.

References

1. M. Yao, Z. Zheng, H. Liu, *Prog. Energy Combust. Sci.* 35-5: 398-437 (2009).
2. Chien, X., Wakai, K., Takahashi, S., Ihara, T., and Shibata, K., *Measurement Science and Technology* 16: 707-715, (2005).
3. Qin, X., Wakai, K., Ihara, T., and Shibara, K., *Journal of the Combustion Society of Japan* (in Japanese) 48-146: 363-371 (2006).
4. Kito, S., Wakai, K., Takahashi, S., Fukaya, N., Komori, K., *Transactions of the JSME, Series B* (in Japanese) 65-633: 303-308 (1999).
5. Wakai, K., Itoh, T., Takahashi, S., Shimizu S., *Transactions of the JSME, Series B* (in Japanese) 65-638: 294-300 (1999).
6. Kito, S., Wakai, K., Takahashi, S., Fukaya, N., Takada, Y., *JSAE Review* 31-2: 373-378 (2000).
7. B Peterson, E Baum, B Bohm, V Sick, A Dreizer, *Proc. of the Combustion Institute*, 34-2, 3653-3660 (2013).
8. F. T.C. Yuen, Ö. L. Gülder, *Proc. of the Combustion Institute*, 32-2, 1747-1754 (2009).
9. D.W. Mattison, J.B. Jeffries, R.K. Hanson, R.R. Steeper, S. De Zilwa, J.E. Dec, M. Sjöberg, W. Hwang, *Proc. of the Combustion Institute*, 31-1, 791-798 (2007).
10. M. Moroto, K. Wakai, S. Takahashi, S. Shimizu, *Combustion Science and Technology* (in Japanese), Vol. 6, pp. 161-170 (1998).
11. M. Moroto, K. Wakai, S. Takahashi, S. Shimizu, *Combustion Science and Technology* (in Japanese), Vol. 7, pp. 175-185 (2000).
12. Grosshandler, W. L., NIST Technical Note (1993).
13. Malkmus, M., *Journal of Optical Society of America*, 53-8: 951-961 (1963).
14. Modest, M. F., *Radiative Heat Transfer*, 2nd Ed., Academic Press, New York: 304-307 (2003).
15. Modest, M. F., Bharadwaj, S. P., *Journal of Quantitative Spectroscopy and Radiative Transfer* 73: 329-338 (2002).
16. Nagae, T., Takahashi, S., Ihara, T., Wakai, K., Urata, Y., Effect of selecting infrared band on temperature measurement in cylinder using infrared pyrometry, *Proc. 44th Symposium (Japanese) on Combustion* (in Japanese) : 42-43 (2006).
17. N. S. Kamarrudin, S. Tanaka, S. Takahashi, T. Ihara, Measurement of Temperature Profile during Ignition Delay in the Cylinder with Fuel Concentration Gradient, *Proc. 9th ASPACC, Gyeongju, CD-ROM*, 121-124 (2013).
18. Ohta, Y., Furutani, M., Kadowaki, S., Terada, K., Takahashi, H., Effect of Mixture Dilution or EGR on Low-Temperature Autoignition under Piston Compression, *COMODIA90*: 111-115 (1990).
19. Konig, G. and Sheppard, C.G.W.: *SAE Trans.* 902135: 820-839 (1990).
20. Curran, H. J., P. Gaffuri, W. J. Pitz, and Westbrook, C. K., *Combustion and Flame* 114: 149-177 (1998).